



# Influence of Fuel to Oxidizer Ratio on Microwave-Assisted Combustion Preparation of Nanostructured KOH/Ca<sub>12</sub>Al<sub>14</sub>O<sub>33</sub> Catalyst Used in Efficient Biodiesel Production

Hamed Nayebzadeh<sup>1\*</sup>, Mohammad Haghghi<sup>2,3\*</sup>, Naser Saghatoleslami<sup>4</sup> and Mohammad Tabasizadeh<sup>5</sup>

## OPEN ACCESS

### Edited by:

Meisam Tabatabaei,  
MARA University of  
Technology, Malaysia

### Reviewed by:

Stefania Specchia,  
Politecnico di Torino, Italy  
Cheng Tung Chong,  
Shanghai Jiao Tong University, China

### \*Correspondence:

Hamed Nayebzadeh  
h.nayebzadeh@esfarayen.ac.ir  
Mohammad Haghghi  
haghghi@sut.ac.ir

### Specialty section:

This article was submitted to  
Bioenergy and Biofuels,  
a section of the journal  
Frontiers in Energy Research

**Received:** 19 February 2020

**Accepted:** 11 May 2020

**Published:** 24 June 2020

### Citation:

Nayebzadeh H, Haghghi M,  
Saghatoleslami N and Tabasizadeh M  
(2020) Influence of Fuel to Oxidizer  
Ratio on Microwave-Assisted  
Combustion Preparation of  
Nanostructured KOH/Ca<sub>12</sub>Al<sub>14</sub>O<sub>33</sub>  
Catalyst Used in Efficient Biodiesel  
Production. *Front. Energy Res.* 8:106.  
doi: 10.3389/fenrg.2020.00106

<sup>1</sup> Faculty of Material and Chemical Engineering, Esfarayen University of Technology, Esfarayen, Iran, <sup>2</sup> Chemical Engineering Faculty, Sahand University of Technology, Tabriz, Iran, <sup>3</sup> Reactor and Catalysis Research Center (RCRC), Sahand University of Technology, Tabriz, Iran, <sup>4</sup> Department of Chemical Engineering, Faculty of Engineering, Ferdowsi University of Mashhad, Mashhad, Iran, <sup>5</sup> Department of Biosystems Engineering, Faculty of Agriculture, Ferdowsi University of Mashhad, Mashhad, Iran

In this study, the microwave-assisted solution combustion method was utilized for the fabrication of Ca<sub>12</sub>Al<sub>14</sub>O<sub>33</sub> as support and the amount of urea was assessed as an important parameter during synthesis of the sample. Synthesized Ca<sub>12</sub>Al<sub>14</sub>O<sub>33</sub> with different fuel amounts was impregnated by KOH and used in the biodiesel production process with canola oil under microwave irradiation. The results presented that the crystallinity, crystalline size, specific surface area, and elemental composition of the final nanocatalysts are affected by the fuel amount. Moreover, during impregnation of potassium components, the structure of support was interestingly transformed from CaAl<sub>2</sub>O<sub>4</sub> to Ca<sub>12</sub>Al<sub>14</sub>O<sub>33</sub> structure due to the incorporation of potassium in an alumina lattice and more diffusion of calcium cations into a support lattice. On the other hand, when the amount of fuel passed the optimum amount (2 times the stoichiometric amount), the crystallinity was reduced due to the formation of high amounts of smoke during combustion and prevention of the entry of air (oxygen) into the system. The results of the microwave-enhanced transesterification reaction confirmed the results of the analyses that the conversion of 94.5% was obtained using an optimum sample at 450 W, 12 molar ratios of methanol/oil, 4 wt.% catalyst, and 60 min reaction time. According to the stability of the optimum sample [at least three times (>75%)], along with its unique mesoporous structure, uniform dispersion of potassium components, and high basicity sites, it can be considered as a comparable solid base nanocatalyst for biodiesel production.

**Keywords:** KOH/Ca<sub>12</sub>Al<sub>14</sub>O<sub>33</sub>, nanostructured catalyst, microwave combustion, biodiesel, canola oil

## INTRODUCTION

Nowadays, the production of renewable, non-toxic, eco-friendly, and environmentally friendly fuels has been of great concern to scientists and governments. Extensive research has been performed on alternative fuels, among which biodiesel has shown its high potential due to its biodegradability, similar properties to petroleum fuel, low emission profiles, excellent lubrication of the engine system, and suitability for industrial production (Mardhiah et al., 2017). Biodiesel, otherwise called fatty acid methyl ester (FAME), is commonly produced via the transesterification of vegetable oil or animal fats with methanol (Dehghani and Haghighi, 2017; Veillette et al., 2017). In fact, the viscosity of feedstocks, which has some drawbacks for engine and injection systems, is reduced by the reaction. The catalyst has an important role in the transesterification reaction, where homogeneous catalysts such as NaOH and KOH are usually utilized (Avhad and Marchetti, 2015). This reaction is carried out in a short time (about 1.5 h), while the separation process for producing the final biodiesel with an appropriate quality takes a long time (Tangy et al., 2016).

Microwave irradiation as a novel technology has been widely considered in chemical reactions (Ajamein and Haghighi, 2016; Rezaee and Haghighi, 2016) and it has been extensively studied in the field of biodiesel production in order to reduce production and separation times. Refaat et al. reported that, in addition to the reduction of the transesterification reaction time (from 75 to 4 min), the separation time was also reduced (from 60 to 3 min) (Refaat and El Sheltawy, 2008). Although microwave irradiation eases the production and separation processes, the major drawback of homogeneous catalysts is that they produce soap, and thus several separation and purification steps are required to obtain pure biodiesel. These processes could cause significant environmental problems, since wastewater is produced by the washing of biodiesel with water several times for the elimination of the soap. Therefore, heterogeneous catalysts have been suggested for biodiesel production, although they have not been meaningfully studied in the microwave system as compared to the conventional heating system (Li et al., 2013; Allami et al., 2019).

Heterogeneous base catalysts have extensively been proposed for biodiesel production; KOH and CaO are often used as an active phase for increasing the basicity of catalysts. Liao and Chung (2013) studied the performance of KOH/CaO in microwave-assisted biodiesel production. However, the low specific surface area and lower stability of CaO as support or during the active phase, due to a simple reaction with H<sub>2</sub>O and CO<sub>2</sub> in the air, are among the issues challenging scientists (de Sousa et al., 2016; Ye et al., 2016). The application of stable basic support was suggested to overcome this problem. Alkali earth aluminates with a general formula M<sub>x</sub>Al<sub>2y</sub>O<sub>x+3y</sub> (M = Mg, Ba, Sr, and Ca) have some unique properties, such as high stability and thermal resistance (Quirino et al., 2016; Naderi and Nayebzadeh, 2019). It seems that calcium sources such as carbonate, nitrate, etc., due to their low prices, are a sufficient component for the preparation of alkali earth aluminate (Gupta and Agarwal, 2016; Roschat et al., 2016).

In previous studies, conventional catalyst preparation methods such as co-precipitation (Meng et al., 2013; Lu et al., 2015) and sol-gel (Selyunina et al., 2013; Mandić and Kurajica, 2015) were utilized for the fabrication of calcium aluminate. Against these long time catalyst preparation processes, the combustion method as a self-propagating high-temperature synthesis (SHS) method shows itself to be a suitable procedure for the preparation of refractory materials with high purity and significantly lower energy and time consumption (González-Cortés and Imbert, 2013; Chang et al., 2014). This method, unlike other catalyst preparation methods, does not require the annealing of final powder at high temperatures (sometimes over 1,000°C) for extended periods of time (Varma et al., 2016; Nayebzadeh et al., 2019). A primary heat is required to initiate the oxidation/reduction reactions, where microwave irradiation has shown to have efficient external heating due to its uniform heating, fast heating rates, and hot spots, as well as selective absorption of radiation by polar substances. This is why it is called microwave combustion synthesis (MCS) (Specchia et al., 2017; Deganello and Tyagi, 2018).

Although the effect of fuel type and other variables on the structure and properties of calcium aluminate fabricated by the MCS method has been studied with our previous work (Nayebzadeh et al., 2016, 2017a,b), further studies can be performed to obtain a sample with the highest activity and stability. Other parameters such as fuel-to-oxidizer, or fuel ratio (FR), microwave irradiation output power, water content in precursor, and pH of the solution have influence on the properties of the final product synthesized by the MCS method (Rosa et al., 2013; Hashemzahi et al., 2020a). Hashemzahi et al. reported that, for preparation of a nanocatalyst with good crystallinity and high activity for biodiesel production, high microwave power must be used (Hashemzahi et al., 2016). Furthermore, it was reported that FR has the greatest influence on the properties and performance of the final powder due to its effect on the temperature of the exothermic combustion reaction during catalyst preparation (Nasiri et al., 2012; Khoshbin et al., 2016) that has not been studied previously. Therefore, in this study, the effect of FR was assessed on the properties of calcium aluminate as support prepared by the MCS method. After impregnation of the potassium component on the surface of supports, their activity was examined in the microwave-enhanced transesterification of canola oil. The samples were characterized using X-ray Diffraction (XRD), Fourier-transform infrared spectroscopy (FTIR), Brunauer-Emmett-Teller (BET), Thermogravimetric (TG), Energy-dispersive X-ray spectroscopy (EDX), Field Emission Scanning Electron Microscopy (FESEM) analyses, and basicity using Hammett indicator. The level of reusability as an optimum aim for industrial use using a catalyst was evaluated for KOH/Ca<sub>12</sub>Al<sub>14</sub>O<sub>33</sub> nanocatalyst fabricated at optimum FR in the biodiesel production process.

## MATERIALS AND METHODS

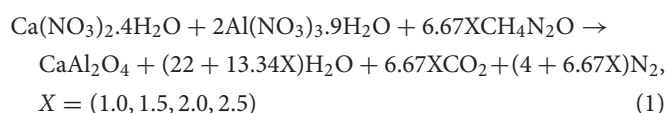
### Materials

Chemical grades of aluminum nitrate (Al(NO<sub>3</sub>)<sub>3</sub>·9H<sub>2</sub>O), calcium nitrate (Ca(NO<sub>3</sub>)<sub>2</sub>·4H<sub>2</sub>O), potassium hydroxide (KOH), urea

(CH<sub>4</sub>N<sub>2</sub>O), and methanol (CH<sub>3</sub>OH) were purchased from Merck. All the materials were used as received without any further purification. The canola oil was supplied from a local store.

## Nanocatalyst Synthesis Procedure

In the MCS method, metal salts such as nitrates are mixed with water and soluble carbohydrates as fuel. In our study, Al(NO<sub>3</sub>)<sub>3</sub>·9H<sub>2</sub>O (20 mmole) and Ca(NO<sub>3</sub>)<sub>2</sub>·6H<sub>2</sub>O (10 mmole) were mixed with 30 mL of deionized water in a beaker and then a desirable amount of urea with 1, 1.5, 2, or 2.5 times of stoichiometric compositions was added. According to propellant chemistry, stoichiometric compositions of the fuel-to-oxidizer ratio were calculated using the total oxidizing and reducing valences of the components (Nayebzadeh et al., 2016). The corresponding chemical reaction for preparation of calcium aluminate with different FRs is shown as follows:



After gelling the mixture by heating at 80°C, the beaker was transformed in the domestic microwave oven (Daewoo, Model No. KOC9N2TB, 900 watts, 2.45 GHz) and irradiated for 10 min. After exhausting the huge amount of gases, the combustion reaction started and the foamy catalyst was produced. The samples were labeled as CA(FR = 1), CA(FR = 1.5), CA(FR = 2), and CA(FR = 2.5).

Potassium components as active phases were impregnated by mixing the supports with the KOH aqueous solution (35 wt.%) and refluxing at 80°C for 2 h. After aging the mixture for 12 h, it was placed in an oven at 110°C overnight to dry. Finally, the powders were calcined at 700°C for 4 h to obtain KCA(FR = 1), KCA(FR = 1.5), KCA(FR = 2), and KCA(FR = 2.5) (Nayebzadeh et al., 2017a). The nanocatalysts synthesis method is shown in **Figure 1**.

## Nanocatalysts Characterization Techniques

XRD analysis was performed to determine the crystalline phase of the samples, where a UNISANTIS/XMD 300 apparatus operating at 45 kV and 80 mA with scanning range of 10–60° by means of Cu K $\alpha$  radiation was utilized. The textural properties of the sample containing a specific surface area, mean pore size, and pore volume were determined using a PHS-1020 (PHSCHINA, China) apparatus by N<sub>2</sub> adsorption/desorption method. TG analysis was utilized for assessing the decomposition of raw materials during catalyst preparation. The phenomenon of microwave combustion reaction was evaluated by TG analysis under air flow in the range of 50–800°C at a heating rate of 20°C/min performed by on an Evolution STA (SETARAM, France) instrument. Using FESEM analysis performed by MIRA3 FEG-SEM (TESCAN, Czech Republic), the morphology and surface structure of the nanocatalysts were assessed. The surface elemental distribution of the samples was depicted by the EDX technique using VEGA II Detector (Czech Republic,

TESCAN). The surface functional groups of the nanocatalysts were assayed by FTIR spectra in the range of 400–4,000 cm<sup>-1</sup> using a SHIMADZU 4300 (Japan) spectrometer. The Hammett indicators method was used to determine the basic strength (H<sub>+</sub>) of the samples where bromothymol blue (H<sub>+</sub> = 7.2), phenolphthalein (H<sub>+</sub> = 9.8), and 2,4-dinitroaniline (H<sub>+</sub> = 15.0) were utilized as indicators. By titration of each color changed mixture containing 0.2 g catalyst, 10 mL methanol, and 1 mL Hammett indicator solution via 0.02 mole benzene carboxylic acid/L anhydrous ethanol solution, the basicity of the nanocatalysts was measured (Ye et al., 2014).

## Experimental Setup for Catalytic Performance Test

The microwave-enhanced transesterification reaction of canola oil was carried out in a 100 mL glass reactor equipped with a water-cooled condenser for assessment of the catalytic activity of the samples. A modified domestic microwave with a hole of 20 mm at its top was utilized to carry out the reaction at microwave output power of 450 W for 1 h. For each reaction, the glass reactor was loaded by 20 g canola oil, 12 mL methanol (12 methanol/oil molar ratios), and 0.8 g catalyst (4 wt.%). Although the reaction was not performed at the optimum conditions, it can provide a suitable conversion for comparing the catalysts. At the end of the reaction, the biodiesel layer mixture was separated from glycerol and used as a catalyst by centrifuging the mixture at 2,500 rpm for 25 min. Its layer was heated to remove excess methanol and obtain pure biodiesel. The conversion of the reaction was determined based on the FAME content of the produced biodiesel. The FAME content of biodiesel was calculated by the following equation:

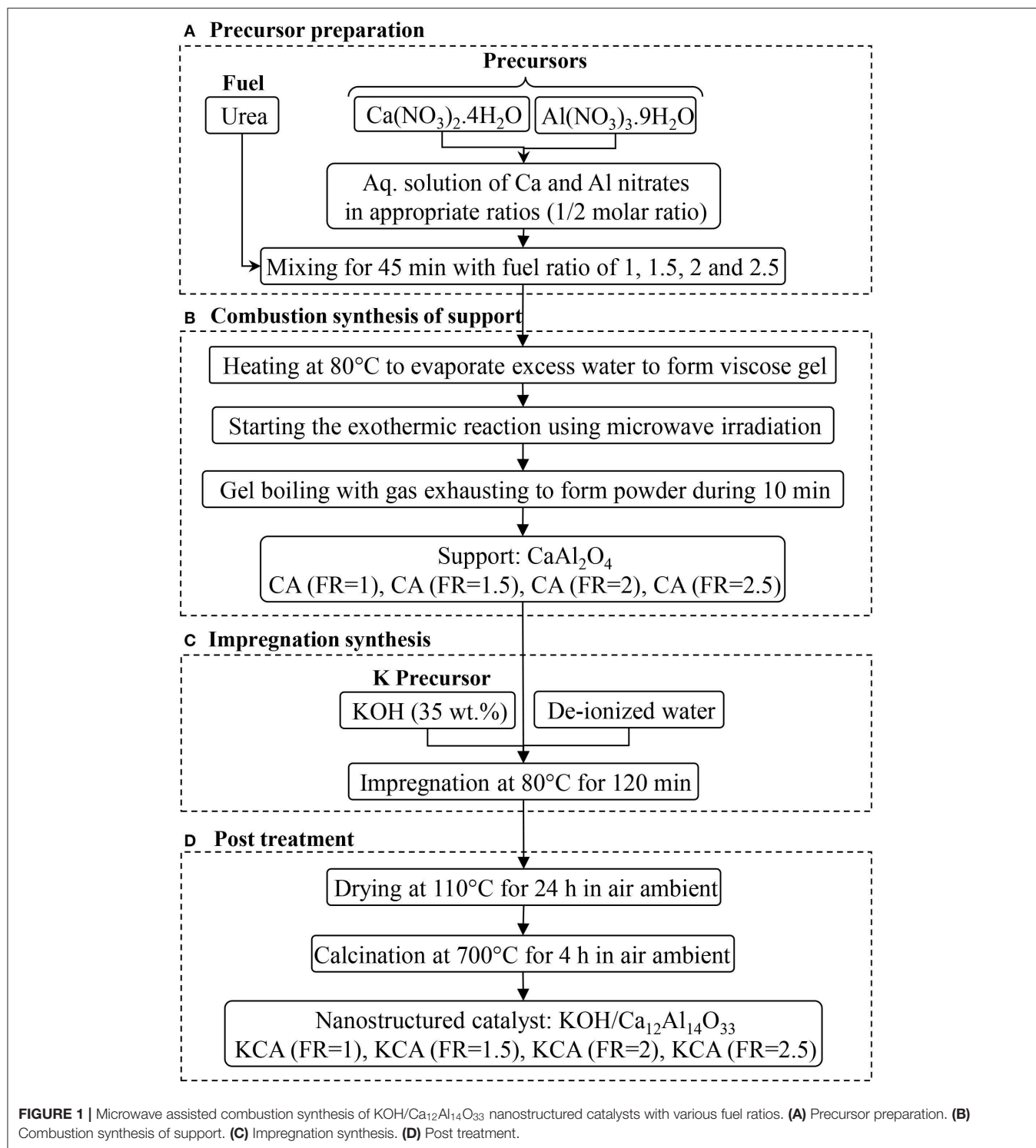
$$\begin{aligned} \text{Conversion (\%)} = \\ \frac{[(\text{area of all FAME} \times \text{weight of reference}) / (\text{area of reference} \\ \times \text{weight of biodiesel sample})] \times 100}{1} \end{aligned} \quad (2)$$

where reference is assigned to methyl non-adeconoate as an internal standard. Area of FAME and reference were mentioned to the area of gas chromatographic (GC; Teif Gostar Faraz co., Iran) peaks of produced biodiesel equipped with FID detector and SUPRAWAX-280 capillary column (30 m × 0.25 mm × 0.25  $\mu$ m).

## RESULTS AND DISCUSSION

### Nanostructured Catalysts Characterization XRD Analysis

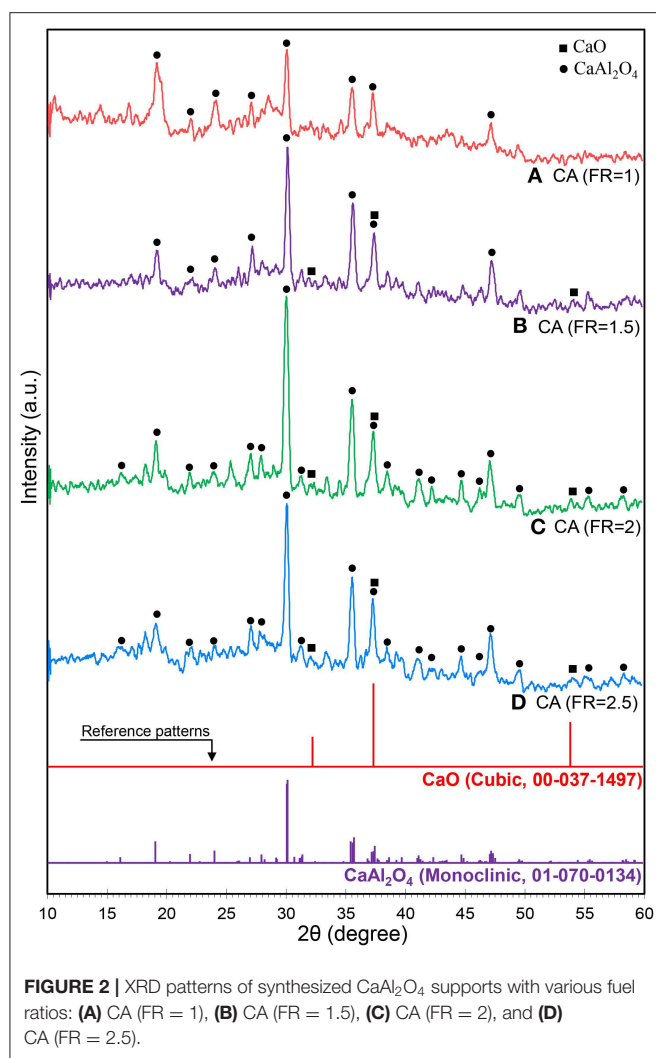
The effect of FR on the crystalline structure of calcium aluminate is illustrated in **Figure 2**. All the samples show the monoclinic phase of the monocalcium aluminate structure (CaAl<sub>2</sub>O<sub>4</sub> as called CA) in accordance with the Joint Committee on Powder Diffraction Standards (JCPDS No. 70-0134) database with different peak intensities. In the CaO and Al<sub>2</sub>O<sub>3</sub> system, mayenite (Ca<sub>12</sub>Al<sub>14</sub>O<sub>33</sub> as called C<sub>12</sub>A<sub>7</sub>) forms as the first structure of calcium aluminate, which quickly reacts with Al<sub>2</sub>O<sub>3</sub> to form CA when sintering temperature and time increase (Nayebzadeh et al., 2017b). Janakova et al. reported that CA is formed at reaction



temperatures up to 1,050°C and higher temperatures are required to have a full crystallinity (Janáková et al., 2007).

The theoretical combustion temperature can be obtained using enthalpy of the reaction and a specific heat capacity of the product when the combustion process assumes adiabatic (Hashemzahi et al., 2020b). If it is assumed that only CaAl<sub>2</sub>O<sub>4</sub>

was formed, the adiabatic combustion temperature obtains 923, 1,263, 1,444, and 1,557°C for a fuel ratio of 1–2.5 (see **Supplementary Material**). It shows that the combustion temperature increased sharply by loading higher amounts of fuel while the rate of temperature increasing reduced at a higher fuel ratio. Moreover, less crystallinity of the sample fabricated at a fuel



ratio of 1 can be proven by the calculated temperature which was under the minimum temperature needed to obtain well crystalline structure of  $\text{CaAl}_2\text{O}_4$  (1,050°C). Thus, it is proven that the temperature of combustion reaction medium is extremely high (Rodríguez et al., 2012). Therefore, the nanocatalysts at the FR above 1.5 contain CaO,  $\text{C}_{12}\text{A}_7$ , CA, and  $\text{Al}_2\text{O}_3$ , with CA being the dominant phase (Rivas Mercury et al., 2005; Ruszak et al., 2011). The diffraction peaks of  $\text{Al}_2\text{O}_3$  (JCPDS No. 76-0144) and  $\text{C}_{12}\text{A}_7$  (JCPDS No. 78-0910) can be, respectively, observed at  $2\theta = 25.4^\circ$  and  $18.1^\circ$ , especially at CA (FR = 2) nanocatalyst.

When the amount of urea increased in the mixture, the burning flame continued from seconds to minutes. An increase of combustion duration caused the formation of the well-defined crystalline structure of CA. The relative crystallinity of the as-prepared CA nanocatalyst, calculated based on the peak at  $2\theta = 30.1^\circ$ , clearly proves the effect of fuel increase on the formation of CA (shown in Table 1). However, the relative crystallinity decreased at a FR of 2.5. Rapid oxygen transport from air to reaction medium is significantly necessary for complete combustion, as in fuel-rich conditions. However,

oxygen diffusion limitations result in incomplete combustion for the CA (FR = 2.5) nanocatalyst (Ghosh et al., 2010). The effect of reaction temperature can be significantly observed in the crystalline size of CA, as the CA (FR = 2) shows the lowest crystalline size (Table 1).

The XRD patterns of the  $\text{KOH}/\text{Ca}_{12}\text{Al}_{14}\text{O}_{33}$  nanocatalyst are shown in Figure 3. It can be clearly observed that the samples were transformed from CA structure to  $\text{C}_{12}\text{A}_7$  phases due to the additional heat treatment and dopant concentration (Avci et al., 2012). The phase transformation is related to the diffusion of  $\text{Ca}^{2+}$  ions through the CA layer to react with  $\text{Al}_2\text{O}_3$  in order to form  $\text{Ca}_3\text{Al}_2\text{O}_6$  ( $\text{C}_3\text{A}$ ) and  $\text{C}_{12}\text{A}_7$ , as the stable phase is finally formed at the expense of CA and  $\text{C}_3\text{A}$  (Tao et al., 2012). In addition, the  $\text{K}_2\text{O}$  (JCPDS No. 22-0493) and  $\text{K}_2\text{CO}_3$  (JCPDS No. 73-0470) phases can be recognized in the XRD patterns of the samples, especially at the KCA (FR = 2) and KCA (FR = 2.5) nanocatalysts. Less amorphous structures in the samples with high crystallinity may allow the potassium component to make individual phases. This phase has a significant effect on the activity of the catalyst in the transesterification reaction (Nayebzadeh et al., 2016).

The relative crystallinity and crystalline size of the samples are also listed in Table 1. The KCA (FR = 2) and KCA (FR = 2.5) nanocatalysts show the highest relative crystallinity and the largest crystalline size, respectively, which might be due to the greater formation of large crystals of  $\text{C}_{12}\text{A}_7$ .

### FTIR Analysis

The FTIR spectra of the  $\text{KOH}/\text{Ca}_{12}\text{Al}_{14}\text{O}_{33}$  nanocatalysts are illustrated in Figure 4. The spectra of all the samples exhibit a bond between 3,200 and 3,400  $\text{cm}^{-1}$ , which is related to O-H stretching vibration of absorbed water molecules on the surface of the nanocatalysts. Moreover, a peak at 1670  $\text{cm}^{-1}$  is also assigned to the bending vibration of water molecules (Khoshbin and Haghghi, 2014; Kazemifard et al., 2019). The characteristic bond in the range of 3,400–3,600  $\text{cm}^{-1}$  can be assigned to Ca/Al-OH groups (Chang et al., 2014). In addition, stretching vibration of Al-O-K groups, due to the attachment of  $\text{K}^+$  ions to alumina, is also observed around 3,600 and 1,100  $\text{cm}^{-1}$ . The bonds at 1,470, 1,395, 1,020, and 935  $\text{cm}^{-1}$  may be associated with the characteristic vibrations of the Al-OH or Al-O-K bonding (Hashemzahi et al., 2016). The characteristic absorption regions of Al-O stretching vibrations for tetrahedral ( $\text{AlO}_4$ ) and octahedral ( $\text{AlO}_6$ ) are, respectively, observed in the 700–850  $\text{cm}^{-1}$  and 500–700  $\text{cm}^{-1}$  (Kazemifard et al., 2018). The tetrahedral bonds of Al-O confirm the formation of  $\text{C}_{12}\text{A}_7$  structure (Lu et al., 2012). The Ca-O bond is observed around 470  $\text{cm}^{-1}$  (Alba-Rubio et al., 2010; Hojjat et al., 2016).

### BET and Basicity Analysis

The BET properties of the samples are listed in Table 1. The specific surface area of the samples sequentially increased from 58.14 to 95.40  $\text{m}^2/\text{g}$  by increasing the FR. This could be due to an increase of the amounts of exhausted gas and combustion time during catalyst preparation. A similar phenomenon was also detected for pore volume and mean pore size of the samples, whereas these decreased by increasing the FR from 2 to 2.5.

**TABLE 1** | Physicochemical properties of synthesized  $\text{CaAl}_2\text{O}_4$  supports and  $\text{KOH}/\text{Ca}_{12}\text{Al}_{14}\text{O}_{33}$  nanostructured catalysts.

Nanocatalyst	BET ( $\text{m}^2/\text{g}$ )	$P_v$ ( $\text{cm}^3$ )	$P_d$ (nm)	Basicity		Relative Crystallinity <sup>a</sup>		Crystallite size <sup>b</sup> (nm)	
				H <sub>-</sub>	Strength (mmol/g)	$\text{CaAl}_2\text{O}_4$	$\text{Ca}_{12}\text{Al}_{14}\text{O}_{33}$	$\text{CaAl}_2\text{O}_4^c$	$\text{Ca}_{12}\text{Al}_{14}\text{O}_{33}^d$
CA(FR = 1)	–	–	–	<7.2	–	42.4	–	25.9	–
CA(FR = 1.5)	–	–	–	<7.2	–	71.2	–	24.9	–
CA(FR = 2)	–	–	–	<7.2	–	100	–	18.5	–
CA(FR = 2.5)	–	–	–	<7.2	–	80.8	–	22.1	–
KCA(FR = 1)	58.14	0.142	5.43	9.8–15	0.392	–	67.4	–	23.3
KCA(FR = 1.5)	62.52	0.304	6.03	9.8–15	0.400	–	92.7	–	25.8
KCA(FR = 2)	64.20	0.441	7.40	9.8–15	0.404	–	100	–	27.5
KCA(FR = 2.5)	95.43	0.314	5.99	9.8–15	0.404	–	100	–	26.9

<sup>a</sup>Relative crystallinity: XRD relative peak intensity at  $2\theta = 30.1^\circ$  for  $\text{CaAl}_2\text{O}_4$  and  $18.1^\circ$  for  $\text{Ca}_{12}\text{Al}_{14}\text{O}_{33}$ .

<sup>b</sup>Crystallite size estimated by Scherrer's equation at  $2\theta = 30.1^\circ$  for  $\text{CaAl}_2\text{O}_4$  and  $18.1^\circ$  for  $\text{Ca}_{12}\text{Al}_{14}\text{O}_{33}$ .

<sup>c</sup>Crystallite phase: Monoclinic (JCPDS: 01-070-0134,  $2\theta = 19.0, 22.0, 23.9, 27.9, 30.1, 35.7, 37.4, 47.2$ ).

<sup>d</sup>Crystallite phase: Cubic (JCPDS: 01-078-910,  $2\theta = 18.1, 27.8, 29.8, 33.4, 36.7, 41.2, 46.7, 55.2, 57.5$ ).

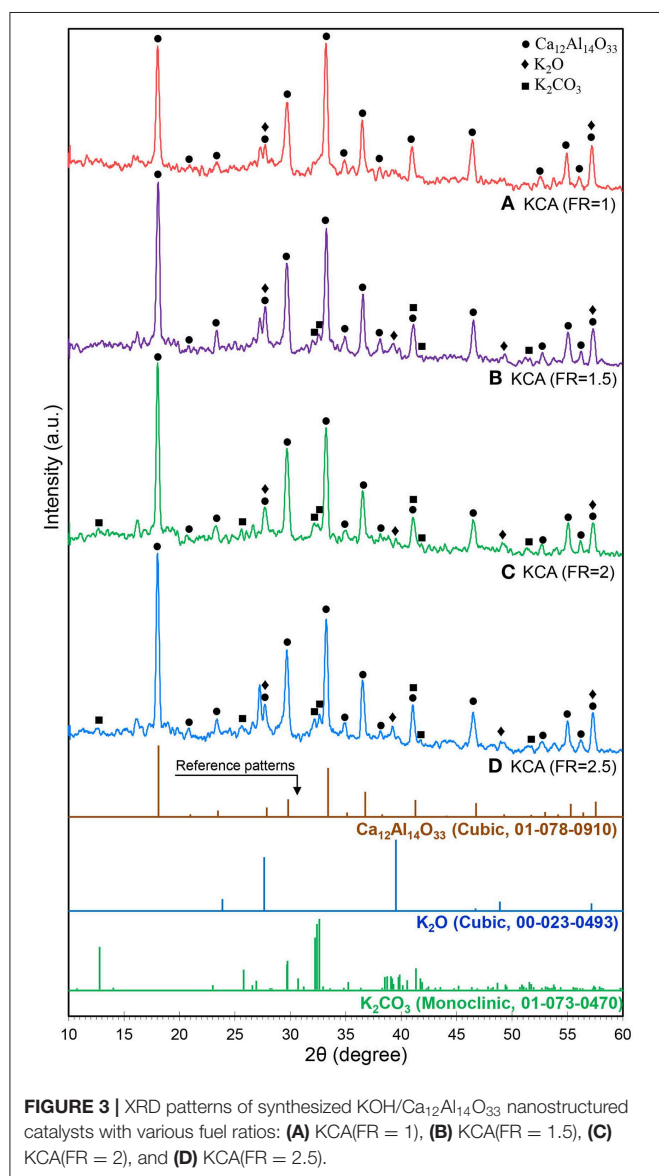


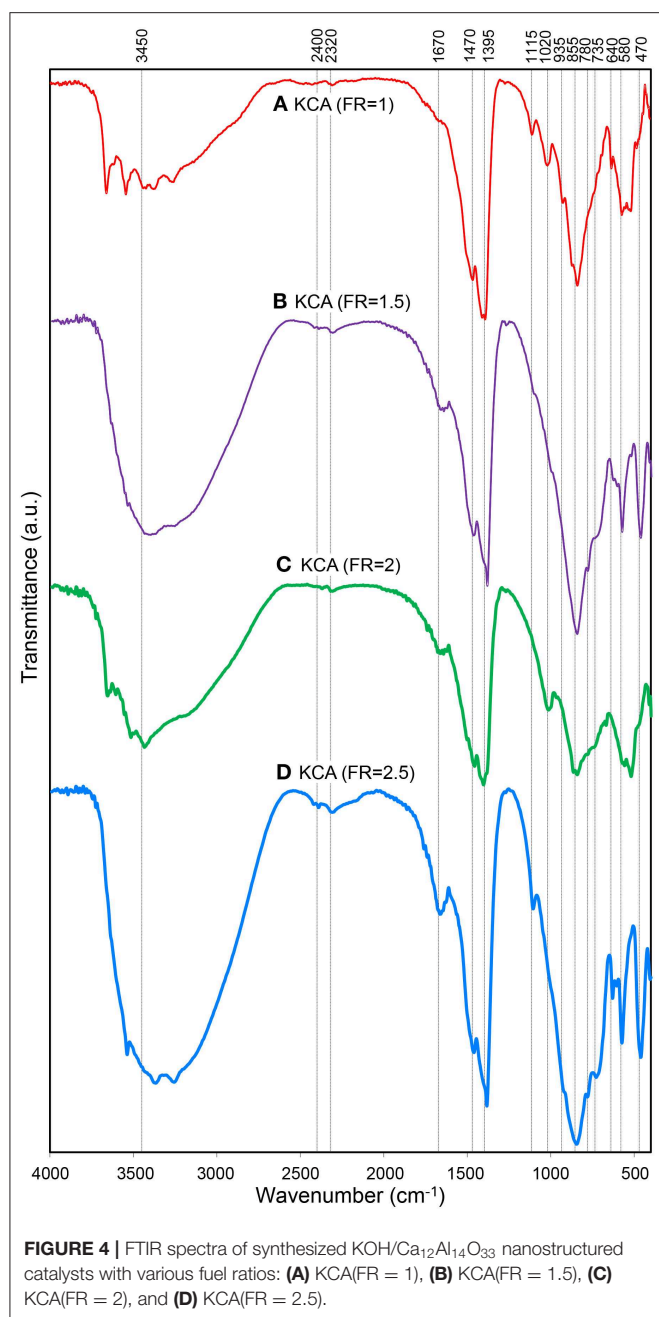
**FIGURE 3** | XRD patterns of synthesized  $\text{KOH}/\text{Ca}_{12}\text{Al}_{14}\text{O}_{33}$  nanostructured catalysts with various fuel ratios: (A) KCA(FR = 1), (B) KCA(FR = 1.5), (C) KCA(FR = 2), and (D) KCA(FR = 2.5).

In the biodiesel production process, porosity of the catalyst can even play a larger role than the surface area. The diffusion of triglycerides molecules into catalyst pores contains seven stages, including: (1) passing through the external film of the catalyst, (2) diffusing into the pores, (3) adsorbing on the active surface, (4) reacting the reactants, (5) disposing the products (biodiesel and glycerol) from the catalyst surface, (6) diffusing toward the outside through the pores, and (7) passing through the external film (Ebadinezhad and Haghghi, 2020). Therefore, the pore size must be insufficient in order to perform the stages 3–7. It was mentioned that the pores must be at least 6 nm in diameter for easy permeation of triglycerides macromolecules (Jacobson et al., 2008). A number of studies have emphasized that restricted diffusion transpires when reactant molecules and pores have comparable dimensions (Lukić et al., 2010). Therefore, triglycerides molecules can easily diffuse through the pores of the major part of the KCA(FR = 2) nanocatalyst, leading to an efficient contact to be established between the reactant and active site. In addition, the KCA(FR = 2) nanocatalyst also shows the largest pores volume.

As shown in **Table 1**, the basicity of the as-prepared catalysts was not meaningfully changed by an increased FR. The basicity is defined as a basic site for a catalyst where KOH plays the most important role in increasing the basic strength. Here, the support (CA) showed insignificant basicity strength in the studied region. Since the amount of impregnated potassium compounds on the catalysts is constant, the samples showed a similar basicity strength.

### TG Analysis

The TG plots of the monocalcium aluminate prepared by different FRs, which explain the level of completing the combustion reaction, are illustrated in **Figure 5**. The weight loss below  $150^\circ\text{C}$  is assigned to the elimination of water from the surface of supports and/or in raw material structure where the CA(FR = 1) showed the highest weight loss (5.5%) (Nayebzadeh et al., 2016). The second reduction in weight in the range of  $150\text{--}500^\circ\text{C}$  is owed to pyrolysis of organic groups



and/or nitrate precursors, which exhibit incomplete combustion reaction (Chen et al., 2014). CA(FR = 1) and CA(FR = 2.5) have high weight loss (around 15%), which is in good agreement with the results of relative crystallinity obtained from the XRD patterns. It confirms that the optimization of the FR in the combustion method is important for obtaining the highest combustion temperature to synthesize the catalyst with a good structure and high crystallinity (Rahmani Vahid and Haghighi, 2016). The last reduction in weight occurred in the range of 500–600°C, which could correspond to the incorporation of calcium components in the alumina lattice to

form CaAl<sub>2</sub>O<sub>4</sub>. Moreover, such a reduction could be attributed to the transition of alumina from the amorphous to crystalline phase, where the CA(FR = 1) illustrates the highest amount of amorphous phases followed by the CA(FR = 1.5) and CA(FR = 2.5) samples with 3.7 and 5.2% weight loss, respectively (Yousefi et al., 2019). The CA(FR = 2) nanocatalyst with 2.5% weight loss confirms that the fuel-to-oxidizer ratio of 2 is an appropriate amount for the preparation of monocalcium aluminate (CaAl<sub>2</sub>O<sub>4</sub>) as support.

### EDX Analysis

The EDX analysis results of the KOH/Ca<sub>12</sub>Al<sub>14</sub>O<sub>33</sub> nanocatalysts (KCAs) are depicted in **Figure 6**. It can be seen that all the samples contain Al, Ca, K, and O elements and no impurity was observed. The KCAs nanocatalysts show similar element distribution percentages of Al, Ca, and K to the parent solution (35.1, 31.8, and 33.1% for Al, Ca, and K, respectively). Due to the increased combustion reaction and increased alumina in the structure with an increasing fuel ratio, the amount of Al element subsequently increased from 29.4% for the KCA(FR = 1) to 40.3% for the KCA(FR = 2.5). Moreover, the potassium component increased with an increase of the FR from 1 to 2 and then was decreased by more fuel loading. This can be related to the extreme increase of the KCA(FR = 2.5) specific surface area that caused the potassium components' distribution to decrease (as seen in **Figure 6D**). The dot-mapping of the samples clearly exhibited that the potassium components were homogeneously dispersed on the surface of support, especially in the KCA(FR = 2) nanocatalyst (**Figure 6C**), which can result in an appropriate activity of the sample.

### FESEM Analysis

The FESEM images of the CA(FR = 2) and KCA(FR = 2) nanocatalysts are illustrated in **Figure 7**. The combustion cavities as external gates provided during the CA(FR = 2) preparation show large diameters in the range of 300–600 nm, and cause the penetration resistance to be reduced for permeation of the reactant (especially large molecules of triglycerides) (Rahmani Vahid and Haghighi, 2016). Moreover, the morphology of the sample shows that the temperature of the combustion reaction was appropriate, such that the particle size with good distribution sizes can be observed. According to a surface particle size distribution histogram, the CA(FR = 2) nanocatalyst shows the size of the particles to be in the range of 5–17 nm with an average size of 11 nm, where the particles with 10–12 nm have the highest frequency.

The KCA(FR = 2) nanocatalyst is shown in the right side of **Figure 7**, in which the morphology of the CA(FR = 2) was not clearly changed by potassium loading. However, the surface particles size distribution was changed; accordingly, the average particle size increased from 11 nm to 12 nm by potassium loading. The results can be proved by the XRD analysis, where the crystalline size increased due to phase transformation from CA to C<sub>12</sub>A<sub>7</sub>. The phase transformation effect on the particle size is due to the increased bond length between Ca, Al, and O in the mayenite structure as compared to monocalcium aluminate.

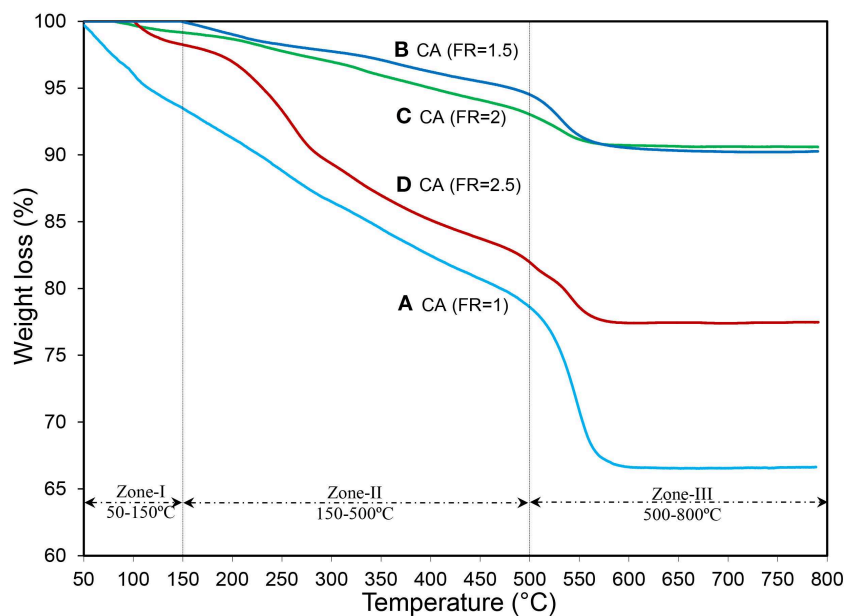


**FIGURE 5** | TG analysis of synthesized  $\text{CaAl}_2\text{O}_4$  supports with various fuel ratios: (A) CA (FR = 1), (B) CA (FR = 1.5), (C) CA (FR = 2), and (D) CA (FR = 2.5).

Minimum and maximum particle sizes of the KCA (FR = 2) nanocatalyst are, respectively, 7.4 and 18.9 nm.

### Catalytic Performance Study Toward Biodiesel Production

The activity of the  $\text{KOH}/\text{Ca}_{12}\text{Al}_{14}\text{O}_{33}$  nanocatalysts is illustrated in **Figure 8**. As expected, the KCA (FR = 2) and KCA (FR = 2.5) nanocatalysts showed higher activity in the conversion of canola oil to biodiesel. The samples showed a high specific surface area and mean pore size, which led to unimpeded permeation of reactants through the porosity of the catalysts, making more contact with their active phases. Moreover, the crystallinity and basicity of these samples were much more than those of the other samples, proving their higher activity. Therefore, the KCA (FR = 2) nanocatalyst was selected as the optimum catalyst and the FR of 2 seemed to be the best ratio for the preparation of calcium aluminate supported by the potassium components.

Dall'Oglio et al. (2014) have conducted a study on the aluminum, calcium, manganese, titanium, and magnesium oxides as support for biodiesel production under microwave irradiation. The results exhibited that alumina was the best support where  $\text{K}_2\text{CO}_3/\text{Al}_2\text{O}_3$  showed the highest activity (98%) at the reaction conditions of methanol/oil molar ratio of 16 and 10 wt.% of the catalyst and reaction time of 30 min. The other potassium precursor showed an intermediate biodiesel conversion. The yield of 60 and 40% was, respectively, obtained using the  $\text{KOH}/\text{Al}_2\text{O}_3$  and  $\text{KI}/\text{Al}_2\text{O}_3$  catalyst in the microwave-assisted biodiesel production. At these conditions, the  $\text{CaO}/\text{Al}_2\text{O}_3$ ,  $\text{CaO}/\text{TiO}_2$ , and  $\text{CaO}/\text{MnO}_2$  catalysts converted 46.2, 36.6, and 49.2% of soybean oil to biodiesel, respectively. This means that the  $\text{Ca}_{12}\text{Al}_{14}\text{O}_{33}$  might be one of the best supports for the loading of active phases for biodiesel production.

### Reusability of KCA (FR = 2) Nanocatalyst in the Biodiesel Production

The reusability of catalysts is an important element in the industrial application of catalysts (Nayebzadeh et al., 2014). To assess the stability of KCA (FR = 2) as an optimum nanocatalyst, it was separated from the reaction mixture after each run by centrifuging the mixture at 6,000 rpm for 20 min and washed with methanol twice time to eliminate the reactants and products from porosities. Then it was dried and calcined at  $700^\circ\text{C}$  for 1 h and reused. The results are presented in **Figure 9**. It can be seen that the catalytic activity of KCA (FR = 2) nanocatalyst decreased from 94.5 to 80.7%, which can be related to leaching and/or poisoning of active phases (potassium components), that can be proven by the brown color of glycerol. However, in the third use, the activity of the catalyst did not meaningfully change and a yield of 76.4% was obtained. The yield slightly decreased with further uses, as a yield of 70.6% was obtained in the fifth run. The results signify that some potassium components have weak bonds with the surface of calcium aluminate as support. The results confirm that the calcium aluminate as support protects its stability during the reaction and could be an appropriate support among those reported so far for loading species for industrial application in the biodiesel production process.

### Comparing the Results With Other Studies

The activity of the samples was compared with other studies as illustrated in **Table 2**.  $\text{KOH}/\text{calcium aluminate}$  presents good activity in the transesterification reaction as high as  $\text{CaO}$  [used in conventional (Ye et al., 2016) or microwave (Hsiao et al., 2011) heating systems]. However,  $\text{CaO}$  can react to methanol to form calcium methoxide in reaction mediums, reduce the

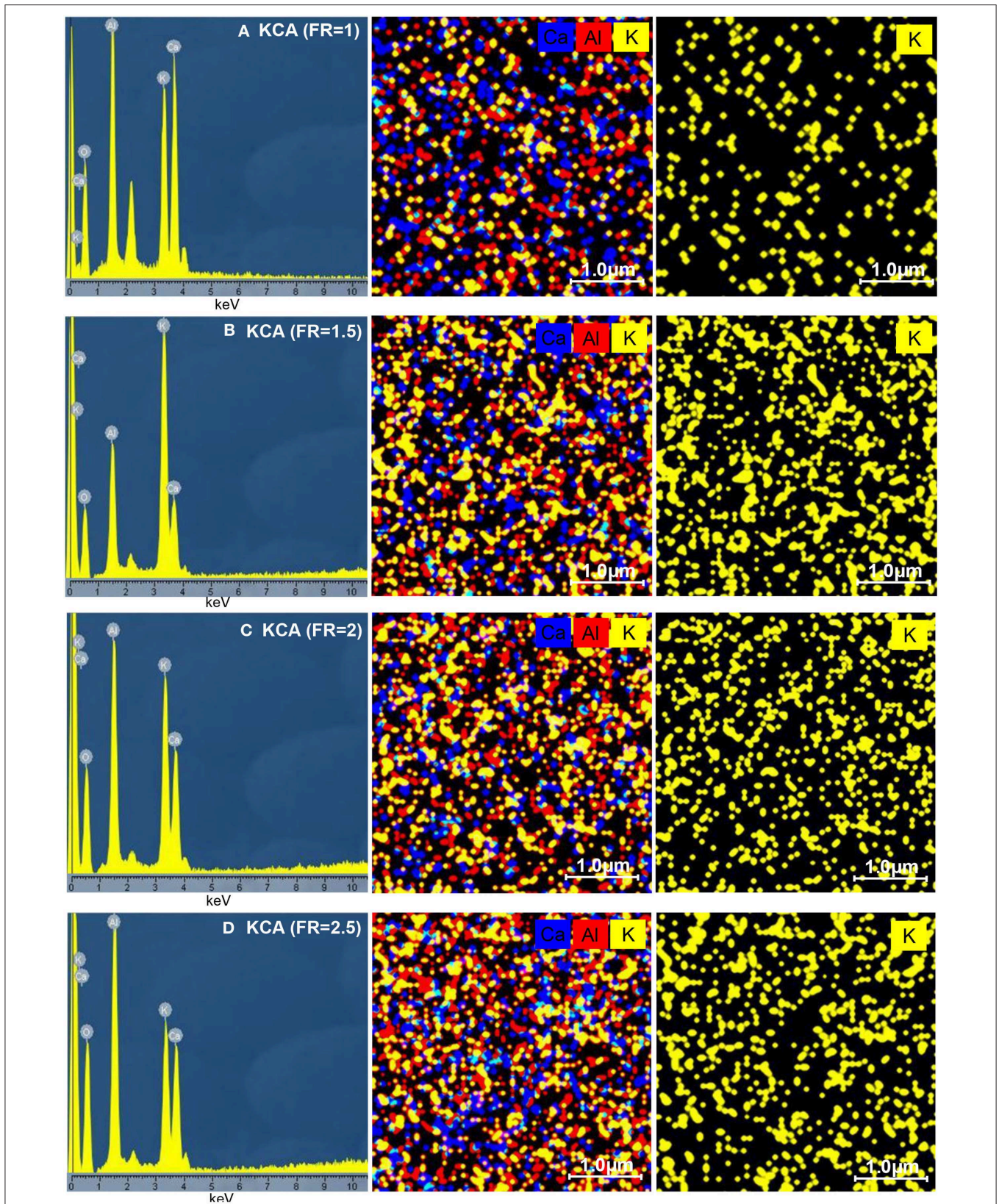
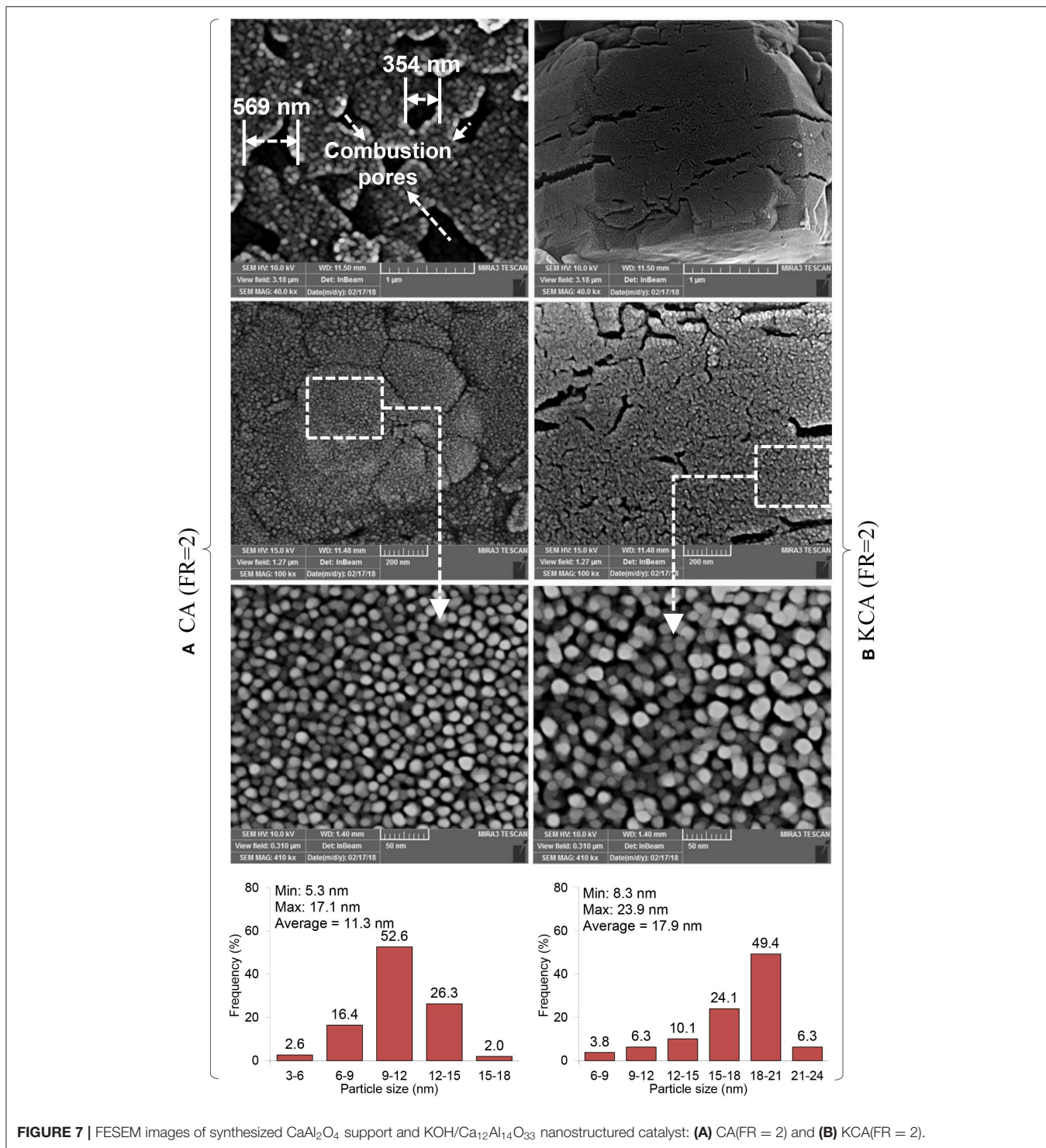
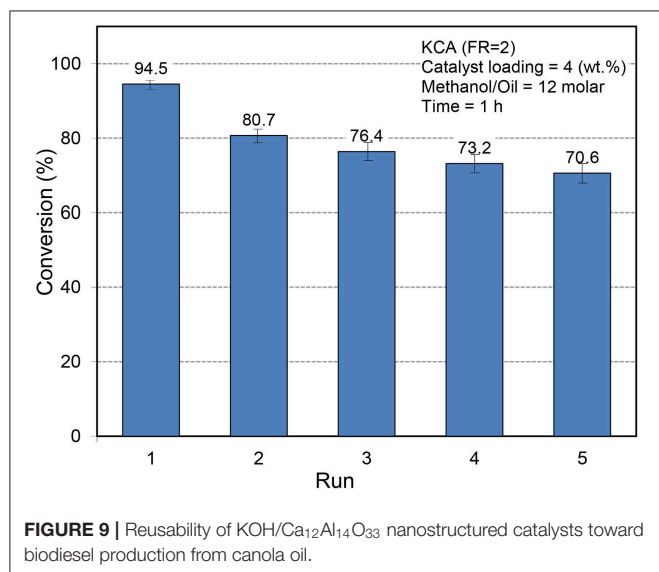
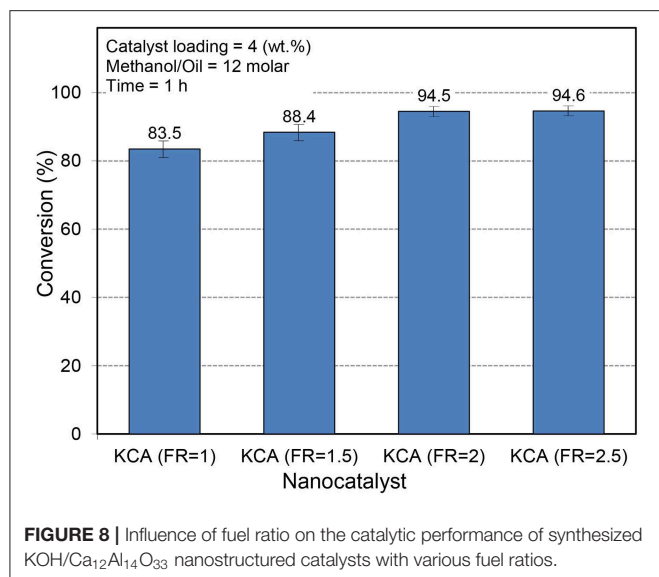


**FIGURE 6** | EDX analysis of synthesized KOH/Ca<sub>12</sub>Al<sub>14</sub>O<sub>33</sub> nanostructured catalysts with various fuel ratios: **(A)** KCA(FR = 1), **(B)** KCA(FR = 1.5), **(C)** KCA(FR = 2), and **(D)** KCA(FR = 2.5).



reaction conversion, and cause high leaching due to the solubility of methanol in a biodiesel layer (de Sousa et al., 2016). Although eggshell as a catalyst, which contains CaO as major material, shows high activity, it was obtained at a high microwave power and duration, or at a high methanol and catalyst concentration (Khemthong et al., 2012; Peng et al., 2018).

The prepared nanocatalyst also presented good activity when the reaction conditions were milder than in other studies. Doping the calcium into an alumina structure can enhance the basicity of the support along with improving the leaching problem of Ca ions reported in previous studies. In addition, the calcium aluminate has different structures that can be studied



to obtain the most active and stable structure for the biodiesel production process.

Moreover, the production procedure is so simple to set up on an industrial scale to reduce the catalyst preparation cost. However, bonding the potassium ions with the surface of the calcium aluminate can be a challenge for enhancing its reusability. It seems that utilizing other types of potassium precursors and the optimization of impregnation conditions may facilitate bonding of K ions with Ca and Al ions, which will be studied in our future work. Therefore, it seems that KOH/calcium aluminate can be further studied to assess its ability to be used for industrial application.

## CONCLUSIONS

CaAl<sub>2</sub>O<sub>4</sub> as alkali calcium aluminate was successfully synthesized by the MCS method, and the effect of fuel amount during the catalyst preparation was assessed. Furthermore, the samples were impregnated by the potassium components to improve their catalytic activity for the transesterification of canola oil to biodiesel through microwave irradiation. The characterization results revealed that the monocalcium aluminate prepared by urea as fuel with twice the stoichiometric amount has a high crystallinity and good precursor decomposition during combustion. This structure was transformed to Ca<sub>12</sub>Al<sub>14</sub>O<sub>33</sub> structure during potassium loading and calcination due to the diffusion of Ca<sup>2+</sup> ions in a monocalcium aluminate lattice and/or reaction of the potassium component with alumina to form potassium aluminate. KOH/Ca<sub>12</sub>Al<sub>14</sub>O<sub>33</sub> showed nanoscale particles where the potassium components were uniformly dispersed on the surface of support. The nanocatalyst, due to its high specific surface area, mean pore size, crystallinity, and basicity, converted high amounts of canola oil to biodiesel through microwave irradiation. The microwave-enhanced biodiesel production was performed under conditions of 450 watts, 12 molar ratio of methanol/oil, 4 wt.% of catalyst, and 1 h reaction time, where a yield of 94.5% was obtained. The nanocatalyst presented a suitable reusability although it required optimizing amounts of the potassium components.

**TABLE 2** | Comparison of catalytic performance of various catalysts in biodiesel production process under microwave irradiation.

Catalyst	Feedstock	Transesterification condition				Yield (%)	References
		Mw. P (W)	MORb	Cc (wt.%)	td (min)		
KOH/calcium aluminate	Soybean	450	12	4	60	94.5	This study
CaO	Soybean	300 (60°C)	7	3	60	96.6	Hsiao et al., 2011
Eggshells (CaO)	WCO	900 (65°C)	9	5	165		Peng et al., 2018
Eggshells (CaO)	Palm	900	18	15	4	96.7	Khemthong et al., 2012
NaOH/ZnO	Soybean	180°C	20	2	180	77.82	Quirino et al., 2017
Ca(OH) <sub>2</sub> /Fe <sub>3</sub> O <sub>4</sub>	Jatropha-Castor	900 (65°C)	12	2	35	95	Chang et al., 2017
CaO	Palm	150	9	5	60	89.9	Ye et al., 2016
SO <sub>3</sub> H-ZnAl <sub>2</sub> O <sub>4</sub>	Palm (esterification)	800 (60°C)	9	1.5	20	94.6	Soltani et al., 2017
Sulfonated activated carbon	Soybean	600 (75°C)	6	20	20	88.7	Rocha et al., 2019
ZrO <sub>2</sub> /Bamboo ash	Soybean	900 (60°C)	15	12	60	96	Fatimah et al., 2019

## DATA AVAILABILITY STATEMENT

The datasets generated for this study are available on request to the corresponding author.

## AUTHOR CONTRIBUTIONS

Conceptualization of the work was done by NS. MH and HN performed the experiments. The graphs and tables were prepared by HN and MH. The results were analyzed by HN, MH, and MT. After writing the manuscript HN, MH, NS, and MT checked its writing quality. All authors contributed to the article and approved the submitted version.

## REFERENCES

- Ajamein, H., and Haghghi, M. (2016). Influence of ambient gas on microwave-assisted combustion synthesis of CuO–ZnO–Al<sub>2</sub>O<sub>3</sub> nanocatalyst used in fuel cell grade hydrogen production via methanol steam reforming. *Ceram. Int.* 42, 17978–17989. doi: 10.1016/j.ceramint.2016.07.092
- Alba-Rubio, A. C., Santamaría-González, J., Mérida-Robles, J. M., Moreno-Tost, R., Martín-Alonso, D., Jiménez-López, A., et al. (2010). Heterogeneous transesterification processes by using CaO supported on zinc oxide as basic catalysts. *Catal. Today* 149, 281–287. doi: 10.1016/j.cattod.2009.06.024
- Allami, H. A., Tabasizadeh, M., Rohani, A., Farzad, A., and Nayebzadeh, H. (2019). Precise evaluation the effect of microwave irradiation on the properties of palm kernel oil biodiesel used in a diesel engine. *J. Clean. Prod.* 241:117777. doi: 10.1016/j.jclepro.2019.117777
- Avci, N., Korthout, K., Newton, M. A., Smet, P. F., and Poelman, D. (2012). Valence states of europium in CaAl<sub>2</sub>O<sub>4</sub>:Eu phosphors. *Opt. Mater. Express* 2, 321–330. doi: 10.1364/OME.2.000321
- Avhad, M. R., and Marchetti, J. M. (2015). A review on recent advancement in catalytic materials for biodiesel production. *Renew. Sustain. Energy Rev.* 50, 696–718. doi: 10.1016/j.rser.2015.05.038
- Chang, K.-L., Lin, Y.-C., Jhang, S.-R., Cheng, W. L., Chen, S.-C., and Mao, S.-Y. (2017). Rapid Jatropa-Castor biodiesel production with microwave heating and a heterogeneous base catalyst nano-Ca(OH)<sub>2</sub>/Fe<sub>3</sub>O<sub>4</sub>. *Catalysts* 7:203. doi: 10.3390/catal7070203
- Chang, Y.-P., Chang, P.-H., Lee, Y.-T., Lee, T.-J., Lai, Y.-H., and Chen, S.-Y. (2014). Morphological and structural evolution of mesoporous calcium aluminate nanocomposites by microwave-assisted synthesis. *Microporous Mesoporous Mater.* 183, 134–142. doi: 10.1016/j.micromeso.2013.09.013
- Chen, J., Jia, L., Guo, X., Xiang, L., and Lou, S. (2014). Production of novel biodiesel from transesterification over KF-modified Ca–Al hydrotalcite catalyst. *RSC Adv.* 4, 60025–60033. doi: 10.1039/C4RA09214G
- Dall'Oglio, E. L., de Sousa, P. T. Jr., de Oliveira, P. T. J., de Vasconcelos, L. G., Parizotto, C. A., and Kuhnen, C. A. (2014). Use of heterogeneous catalysts in methylic biodiesel production induced by microwave irradiation. *Química Nova* 37, 411–417. doi: 10.5935/0100-4042.20140081
- de Sousa, F. P., dos Reis, G. P., Cardoso, C. C., Mussel, W. N., and Pasa, V. M. D. (2016). Performance of CaO from different sources as a catalyst precursor in soybean oil transesterification: Kinetics and leaching evaluation. *J. Environ. Chem. Eng.* 4, 1970–1977. doi: 10.1016/j.jece.2016.03.009
- Deganello, F., and Tyagi, A. K. (2018). Solution combustion synthesis, energy and environment: Best parameters for better materials. *Progress Cryst. Growth Character. Mater.* 64, 23–61. doi: 10.1016/j.pcrysgrow.2018.03.001
- Dehghani, S., and Haghghi, M. (2017). Sono-sulfated zirconia nanocatalyst supported on MCM-41 for biodiesel production from sunflower oil: influence of ultrasound irradiation power on catalytic properties and performance. *Ultras. Sonochem.* 35, 142–151. doi: 10.1016/j.ulsonch.2016.09.012
- Ebadinezhad, B., and Haghghi, M. (2020). Sono-solvothermal decoration of pore size controlled SAPO-34 by nano-ceria for green fuel production via esterification reaction. *Chem. Eng. J.* 125146. doi: 10.1016/j.cej.2020.125146

## FUNDING

The authors gratefully acknowledge Esfarayen University of Technology (grant number: 93/9311), Ferdowsi University of Mashhad (grant number: 32009), and Sahand University of Technology for the financial support of the research as well as Iran Nanotechnology Initiative Council for complementary financial supports (grant number: 80968).

## SUPPLEMENTARY MATERIAL

The Supplementary Material for this article can be found online at: <https://www.frontiersin.org/articles/10.3389/fenrg.2020.00106/full#supplementary-material>

- Fatimah, I., Rubiyanto, D., Taushiyah, A., Najah, F. B., Azmi, U., and Sim, Y.-L. (2019). Use of ZrO<sub>2</sub> supported on bamboo leaf ash as a heterogeneous catalyst in microwave-assisted biodiesel conversion. *Sustain. Chem. Pharm.* 12:100129. doi: 10.1016/j.scp.2019.100129
- Ghosh, S. K., Prakash, A., Datta, S., Roy, S. K., and Basu, D. (2010). Effect of fuel characteristics on synthesis of calcium hydroxyapatite by solution combustion route. *Bull. Mater. Sci.* 33, 7–16. doi: 10.1007/s12034-010-0010-3
- González-Cortés, S. L., and Imbert, F. E. (2013). Fundamentals, properties and applications of solid catalysts prepared by solution combustion synthesis (SCS). *Appl. Catal. A General* 452, 117–131. doi: 10.1016/j.apcata.2012.11.024
- Gupta, J., and Agarwal, M. (2016). Preparation and characterization of CaO nanoparticle for biodiesel production. *AIP Confer. Proc.* 1724:020066. doi: 10.1063/1.4945186
- Hashemzahi, M., Pirouzfard, V., Nayebzadeh, H., and Alihosseini, A. (2020a). Effect of synthesizing conditions on the activity of zinc-copper aluminate nanocatalyst prepared by microwave combustion method used in the esterification reaction. *Fuel* 263:116422. doi: 10.1016/j.fuel.2019.116422
- Hashemzahi, M., Pirouzfard, V., Nayebzadeh, H., and Alihosseini, A. (2020b). Application of response surface methodology to optimize high active Cu–Zn–Al mixed metal oxide fabricated via microwave-assisted solution combustion method. *Adv. Powder Technol.* 31, 1470–1479. doi: 10.1016/j.apt.2020.01.010
- Hashemzahi, M., Saghatoleslami, N., and Nayebzadeh, H. (2016). A study on the structure and catalytic performance of Zn<sub>x</sub>Cu<sub>1-x</sub>Al<sub>2</sub>O<sub>4</sub> catalysts synthesized by the solution combustion method for the esterification reaction. *Comptes Rendus Chim.* 19, 955–962. doi: 10.1016/j.crci.2016.05.006
- Hojjat, M., Nayebzadeh, H., Khadangi-Mahrood, M., and Rahmani-Vahid, B. (2016). Optimization of process conditions for biodiesel production over CaO–Al<sub>2</sub>O<sub>3</sub>/ZrO<sub>2</sub> catalyst using response surface methodology. *Chem. Papers* 71, 689–698. doi: 10.1007/s11696-016-0096-1
- Hsiao, M.-C., Lin, C.-C., and Chang, Y.-H. (2011). Microwave irradiation-assisted transesterification of soybean oil to biodiesel catalyzed by nanopowder calcium oxide. *Fuel* 90, 1963–1967. doi: 10.1016/j.fuel.2011.01.004
- Jacobson, K., Gopinath, R., Meher, L. C., and Dalai, A. K. (2008). Solid acid catalyzed biodiesel production from waste cooking oil. *Appl. Catal. B Environ.* 85, 86–91. doi: 10.1016/j.apcatb.2008.07.005
- Janáková, S., Salavcová, L., Renaudin, G., Filinchuk, Y., Boyer, D., and Boutinaud, P. (2007). Preparation and structural investigations of sol–gel derived -doped. *J. Phys. Chem. Solids* 68, 1147–1151. doi: 10.1016/j.jpcc.2006.12.034
- Kazemifard, S., Nayebzadeh, H., Saghatoleslami, N., and Safakish, E. (2018). Assessment the activity of magnetic KOH/Fe<sub>3</sub>O<sub>4</sub>@Al<sub>2</sub>O<sub>3</sub> core–shell nanocatalyst in transesterification reaction: effect of Fe/Al ratio on structural and performance. *Environ. Sci. Pollut. Res.* 25, 32811–32821. doi: 10.1007/s11356-018-3249-7
- Kazemifard, S., Nayebzadeh, H., Saghatoleslami, N., and Safakish, E. (2019). Application of magnetic alumina-ferric oxide nanocatalyst supported by KOH for in-situ transesterification of microalgae cultivated in wastewater medium. *Biomass Bioener.* 129:105338. doi: 10.1016/j.biombioe.2019.105338
- Khemthong, P., Luadthong, C., Nualpaeng, W., Changsuwan, P., Tongprem, P., Viriya-empikul, N., et al. (2012). Industrial eggshell wastes as the heterogeneous

- catalysts for microwave-assisted biodiesel production. *Catal. Today* 190, 112–116. doi: 10.1016/j.cattod.2011.12.024
- Khoshbin, R., and Haghghi, M. (2014). Direct conversion of syngas to dimethyl ether as a green fuel over ultrasound-assisted synthesized CuO-ZnO-Al<sub>2</sub>O<sub>3</sub>/HZSM-5 nanocatalyst: effect of active phase ratio on physicochemical and catalytic properties at different process conditions. *Catal. Sci. Technol.* 4, 1779–1792. doi: 10.1039/C3CY01089A
- Khoshbin, R., Haghghi, M., and Margan, P. (2016). Combustion dispersion of CuO-ZnO-Al<sub>2</sub>O<sub>3</sub> nanocatalyst over HZSM-5 used in DME production as a green fuel: effect of citric acid to nitrate ratio on catalyst properties and performance. *Energy Convers. Manage.* 120, 1–12. doi: 10.1016/j.enconman.2016.04.076
- Li, Y., Ye, B., Shen, J., Tian, Z., Wang, L., Zhu, L., et al. (2013). Optimization of biodiesel production process from soybean oil using the sodium potassium tartrate doped zirconia catalyst under microwave chemical reactor. *Bioresour. Technol.* 137, 220–225. doi: 10.1016/j.biortech.2013.03.126
- Liao, C.-C., and Chung, T.-W. (2013). Optimization of process conditions using response surface methodology for the microwave-assisted transesterification of Jatropha oil with KOH impregnated CaO as catalyst. *Chem. Eng. Res. Design* 91, 2457–2464. doi: 10.1016/j.cherd.2013.04.009
- Lu, S., Chunfeng, H., Yoshio, S., and Qing, H. (2012). Study of phase transformation behaviour of alumina through precipitation method. *J. Phys. D Appl. Phys.* 45:215302. doi: 10.1088/0022-3727/45/21/215302
- Lu, Y., Zhang, Z., Xu, Y., Liu, Q., and Qian, G. (2015). CaFeAl mixed oxide derived heterogeneous catalysts for transesterification of soybean oil to biodiesel. *Bioresour. Technol.* 190, 438–441. doi: 10.1016/j.biortech.2015.02.046
- Lukić, I., Krstić, J., Glišić, S., Jovanović, D., and Skala, D. (2010). Biodiesel synthesis using K<sub>2</sub>CO<sub>3</sub>/Al-O-Si aerogel catalysts. *J. Serbian Chem. Soc.* 75, 789–801. doi: 10.2298/JSC090707047L
- Mandić, V., and Kurajica, S. (2015). The influence of solvents on sol-gel derived calcium aluminate. *Mater. Sci. Semiconductor Process.* 38, 306–313. doi: 10.1016/j.mssp.2015.01.004
- Mardhiah, H. H., Ong, H. C., Masjuki, H. H., Lim, S., and Lee, H. V. (2017). A review on latest developments and future prospects of heterogeneous catalyst in biodiesel production from non-edible oils. *Renew. Sustain. Energy Rev.* 67, 1225–1236. doi: 10.1016/j.rser.2016.09.036
- Meng, Y.-L., Wang, B.-Y., Li, S.-F., Tian, S.-J., and Zhang, M.-H. (2013). Effect of calcination temperature on the activity of solid Ca/Al composite oxide-based alkaline catalyst for biodiesel production. *Bioresour. Technol.* 128, 305–309. doi: 10.1016/j.biortech.2012.10.152
- Naderi, F., and Nayebzadeh, H. (2019). Performance and stability assessment of Mg-Al-Fe nanocatalyst in the transesterification of sunflower oil: effect of Al/Fe molar ratio. *Indus. Crops Prod.* 141:111814. doi: 10.1016/j.indcrop.2019.111814
- Nasiri, H., Bahrami Motlagh, E., Vahdati Khaki, J., and Zebarjad, S. M. (2012). Role of fuel/oxidizer ratio on the synthesis conditions of Cu-Al<sub>2</sub>O<sub>3</sub> nanocomposite prepared through solution combustion synthesis. *Mater. Res. Bull.* 47, 3676–3680. doi: 10.1016/j.materresbull.2012.06.041
- Nayebzadeh, H., Saghatoleslami, N., Haghghi, M., and Tabasizadeh, M. (2017b). Influence of fuel type on microwave-enhanced fabrication of KOH/Ca<sub>12</sub>Al<sub>14</sub>O<sub>33</sub> nanocatalyst for biodiesel production via microwave heating. *J. Taiwan Inst. Chem. Eng.* 75, 148–155. doi: 10.1016/j.jtice.2017.03.018
- Nayebzadeh, H., Saghatoleslami, N., Haghghi, M., and Tabasizadeh, M. (2019). Catalytic activity of KOH-CaO-Al<sub>2</sub>O<sub>3</sub> nanocomposites in biodiesel production: impact of preparation method. *Int. J. Self Propagat. High Temp. Synth.* 28, 18–27. doi: 10.3103/S1061386219010102
- Nayebzadeh, H., Saghatoleslami, N., Maskooki, A., and Vahid, B. R. (2014). Preparation of supported nanosized sulfated zirconia by strontia and assessment of its activities in the esterification of oleic acid. *Chem. Biochem. Eng. Q.* 25, 259–265. doi: 10.15255/CABEQ.2013.1894
- Nayebzadeh, H., Saghatoleslami, N., and Tabasizadeh, M. (2016). Optimization of the activity of KOH/calcium aluminate nanocatalyst for biodiesel production using response surface methodology. *J. Taiwan Inst. Chem. Eng.* 68, 379–386. doi: 10.1016/j.jtice.2016.09.041
- Nayebzadeh, H., Saghatoleslami, N., and Tabasizadeh, M. (2017a). Application of microwave irradiation for preparation of a KOH/calcium aluminate nanocatalyst and biodiesel. *Chem. Eng. Technol.* 40, 1826–1834. doi: 10.1002/ceat.201600466
- Peng, Y.-P., Amesho, K. T. T., Chen, C.-E., Jhang, S.-R., Chou, F.-C., and Lin, Y.-C. (2018). Optimization of biodiesel production from waste cooking oil using waste eggshell as a base catalyst under a microwave heating system. *Catalysts* 8:81. doi: 10.3390/catal8020081
- Quirino, M. R., Oliveira, M. J. C., Keyson, D., Lucena, G. L., Oliveira, J., and Gama, L. (2016). Synthesis of zinc aluminate with high surface area by microwave hydrothermal method applied in the transesterification of soybean oil (biodiesel). *Mater. Res. Bull.* 74, 124–128. doi: 10.1016/j.materresbull.2015.10.027
- Quirino, M. R., Oliveira, M. J. C., Keyson, D., Lucena, G. L., Oliveira, J., and Gama, L. (2017). Synthesis of zinc oxide by microwave hydrothermal method for application to transesterification of soybean oil (biodiesel). *Mater. Chem. Phys.* 185, 24–30. doi: 10.1016/j.matchemphys.2016.09.062
- Rahmani Vahid, B., and Haghghi, M. (2016). Urea-nitrate combustion synthesis of MgO/MgAl<sub>2</sub>O<sub>4</sub> nanocatalyst used in biodiesel production from sunflower oil: Influence of fuel ratio on catalytic properties and performance. *Energy Convers. Manage.* 126, 362–372. doi: 10.1016/j.enconman.2016.07.050
- Refaat, A. A., and El Sheltawy, S. T. (2008). Time factor in microwave-enhanced biodiesel production. *WSEAS Trans. Environ. Dev.* 4, 279–288.
- Rezaee, L., and Haghghi, M. (2016). Citrate complexation microwave assisted synthesis of Ce<sub>0.8</sub>Zr<sub>0.2</sub>O<sub>2</sub> nanocatalyst over Al<sub>2</sub>O<sub>3</sub> used in CO oxidation for hydrogen purification: influence of composite loading and synthesis method. *RSC Adv.* 6, 34055–34065. doi: 10.1039/C6RA02973F
- Rivas Mercury, J. M., De Aza, A. H., and Pena, P. (2005). Synthesis of CaAl<sub>2</sub>O<sub>4</sub> from powders: Particle size effect. *J. Eur. Ceram. Soc.* 25, 3269–3279. doi: 10.1016/j.jeurceramsoc.2004.06.021
- Rocha, P. D., Oliveira, L. S., and Franca, A. S. (2019). Sulfonated activated carbon from corn cobs as heterogeneous catalysts for biodiesel production using microwave-assisted transesterification. *Renew. Energy* 143, 1710–1716. doi: 10.1016/j.renene.2019.05.070
- Rodriguez, M. A., Aguilar, C. L., and Aghayan, M. A. (2012). Solution combustion synthesis and sintering behavior of CaAl<sub>2</sub>O<sub>4</sub>. *Ceram. Int.* 38, 395–399. doi: 10.1016/j.ceramint.2011.07.020
- Rosa, R., Veronesi, P., and Leonelli, C. (2013). A review on combustion synthesis intensification by means of microwave energy. *Chem. Eng. Process. Process Intensific.* 71, 2–18. doi: 10.1016/j.cep.2013.02.007
- Roschat, W., Siritanon, T., Yoosuk, B., and Promarak, V. (2016). Biodiesel production from palm oil using hydrated lime-derived CaO as a low-cost basic heterogeneous catalyst. *Energy Convers. Manage.* 108, 459–467. doi: 10.1016/j.enconman.2015.11.036
- Ruszkak, M., Witkowski, S., Pietrzyk, P., Kotarba, A., and Sojka, Z. (2011). The role of intermediate calcium aluminate phases in solid state synthesis of mayenite (Ca<sub>12</sub>Al<sub>14</sub>O<sub>33</sub>). *Funct. Mater. Lett.* 4, 183–186. doi: 10.1142/S1793604711001907
- Selyunina, L. A., Mishenina, L. N., Slizhov, Y. G., and Kozik, V. V. (2013). Effect of citric acid and ethylene glycol on the formation of calcium aluminate via the sol-gel method. *Russian J. Inorgan. Chem.* 58, 450–455. doi: 10.1134/S0036023613040165
- Soltani, S., Rashid, U., Nehdi, I. A., Al-Resayes, S. I., and Al-Muhtaseb, A. A. H. (2017). Sulfonated mesoporous zinc aluminate catalyst for biodiesel production from high free fatty acid feedstock using microwave heating system. *J. Taiwan Inst. Chem. Eng.* 70, 219–228. doi: 10.1016/j.jtice.2016.10.054
- Specchia, S., Ercolino, G., Karimi, S., Italiano, C., and Vita, A. (2017). Solution combustion synthesis for preparation of structured catalysts: a mini-review on process intensification for energy applications and pollution control. *Int. J. Self Propagat. High Temp. Synth.* 26, 166–186. doi: 10.3103/S1061386217030062
- Tangy, A., Pulidindi, I. N., and Gedanken, A. (2016). SiO<sub>2</sub> beads decorated with SrO nanoparticles for biodiesel production from waste cooking oil using microwave irradiation. *Energy Fuels* 30, 3151–3160. doi: 10.1021/acs.energyfuels.6b00256
- Tao, G., Hua, Z., Gao, Z., Chen, Y., Wang, L., He, Q., et al. (2012). Synthesis and catalytic activity of mesostructured KF/CaxAl<sub>2</sub>O<sub>(x+3)</sub> for the transesterification reaction to produce biodiesel. *RSC Adv.* 2, 12337–12345. doi: 10.1039/c2ra22218c
- Varma, A., Mukasyan, A. S., Rogachev, A. S., and Manukyan, K. V. (2016). Solution combustion synthesis of nanoscale materials. *Chem. Rev.* 116, 14493–14586. doi: 10.1021/acs.chemrev.6b00279

- Veillette, M., Giroir-Fendler, A., Faucheux, N., and Heitz, M. (2017). Esterification of free fatty acids with methanol to biodiesel using heterogeneous catalysts: from model acid oil to microalgae lipids. *Chem. Eng. J.* 308, 101–109. doi: 10.1016/j.cej.2016.07.061
- Ye, B., Qiu, F., Sun, C., Li, Y., and Yang, D. (2014). Biodiesel production from soybean oil using heterogeneous solid base catalyst. *J. Chem. Technol. Biotechnol.* 89, 988–997. doi: 10.1002/jctb.4190
- Ye, W., Gao, Y., Ding, H., Liu, M., Liu, S., Han, X., et al. (2016). Kinetics of transesterification of palm oil under conventional heating and microwave irradiation, using CaO as heterogeneous catalyst. *Fuel* 180, 574–579. doi: 10.1016/j.fuel.2016.04.084
- Yousefi, S., Haghghi, M., and Rahmani Vahid, B. (2019). Role of glycine/nitrates ratio on structural and texture evolution of MgO-based nanocatalyst fabricated by hybrid microwave-impregnation method for biofuel production. *Energy Convers. Manage.* 182, 251–261. doi: 10.1016/j.enconman.2018.12.067

**Conflict of Interest:** The authors declare that the research was conducted in the absence of any commercial or financial relationships that could be construed as a potential conflict of interest.

Copyright © 2020 Nayebzadeh, Haghghi, Saghatoleslami and Tabasizadeh. This is an open-access article distributed under the terms of the Creative Commons Attribution License (CC BY). The use, distribution or reproduction in other forums is permitted, provided the original author(s) and the copyright owner(s) are credited and that the original publication in this journal is cited, in accordance with accepted academic practice. No use, distribution or reproduction is permitted which does not comply with these terms.